

## BEHAVIOUR OF A LEAD COLLIMATOR FOR A GAMMA-RAY TELESCOPE EXPOSED TO GAMMA RADIATION IN THE ENERGY RANGE 1–100 MeV

I.N. Azcárate<sup>1</sup>

Instituto Argentino de Radioastronomía

and

V.J. Mugheri

Comisión Nacional de Actividades Espaciales  
Argentina

*Received 1995 November 29; accepted 1996 June 21*

### RESUMEN

Se aplica el método de Monte Carlo para estudiar la transmisión de la radiación gama en el rango de energías 1–100 MeV a través de un colimador de plomo que fue parte de un telescopio de rayos gama. El cálculo da el espectro continuo y la intensidad de la línea de 511 keV, que emergen de la cara interna del colimador como resultado de las interacciones electromagnéticas múltiples que ocurren en su interior. Se discute también el fondo resultante del decaimiento de núcleos radioactivos generados por interacciones nucleares (fragmentación) de los rayos cósmicos y captura de neutrones en el plomo. Los resultados globales muestran, que el fondo instrumental no reduce significativamente la sensibilidad del detector respecto a la esperada para un colimador idealmente “limpio”.

### ABSTRACT

The Monte Carlo method is applied to study the transmission of a lead collimator 3 cm thick to gamma radiation in the energy range 1–100 MeV, which was part of a  $\gamma$ -ray telescope. The computation gives the continuum spectrum and the 511 keV line intensity emerging from the inner face of the collimator as the result of the electromagnetic interactions occurring inside it. We also discuss the resulting background from the decay of the radioactive nuclei generated by the nuclear interactions (spallation) of cosmic rays, and neutron capture in lead. The overall results show that the induced instrumental background does not significantly reduce the detector sensitivity as compared to that expected of an ideally “clean” collimator.

*Key words:* **ATMOSPHERIC EFFECTS — GAMMA RAYS-OBSERVATIONS — INSTRUMENTATION-DETECTORS**

### 1. INTRODUCTION

Gamma-ray astronomy provides a unique channel to study high-energy particle and nuclear processes throughout the Universe. However, as a direct con-

sequence of the extreme energy of the photons, in spite of the fact that their luminosity content from a given source may be high, their flux numbers at Earth are generally low. Furthermore,  $\gamma$ -ray telescopes are obliged to operate either near the top of the Earth's atmosphere or on a space platform. In either case they encounter an intense radiation environment, such that  $\gamma$ -ray astronomical observations are in general performed under low signal-to-noise

<sup>1</sup> Member of the Carrera del Investigador Científico y Tecnológico del Consejo Nacional de Investigaciones Científicas y Técnicas, (CONICET), Argentina.

ratio conditions and require long observation periods to obtain statistically meaningful measurements. In particular, for balloon flown  $\gamma$ -ray detectors, the atmospheric background may be considerable and affects the sensitivity of the observations. A suitable collimator, by reducing the effective aperture of the detector system, may reduce the atmospheric background but, in turn, being exposed to the various components of the secondary cosmic radiation, may also produce instrumental background gamma radiation in the considered energy range.

In this paper, a study is made of the behaviour of a lead collimator when exposed to gamma radiation in the energy range 1–100 MeV. This study was used to estimate the instrumental background contribution to the counting rate in a  $\gamma$ -ray detector system whose main part was a NaI (Tl) crystal and which is described in the next section.

## 2. DETECTOR SYSTEM

The main detector (Figure 1) was a NaI (Tl) scintillator of 5.1 cm diameter and 3.8 cm height, partially surrounded by a Pb collimator 3 cm thick. The collimator, in turn, was enclosed by two layers of plastic scintillator, 1 cm thick. The external scintillator was coupled to an EMI 9530 photomultiplier, whose output was in anticoincidence with that corresponding to the central scintillator, to eliminate from the spectral analysis the pulses originated by charged particles traversing both the external and central scintillator.

The lead collimator attenuates almost completely the gamma radiation up to about 400 keV, being the

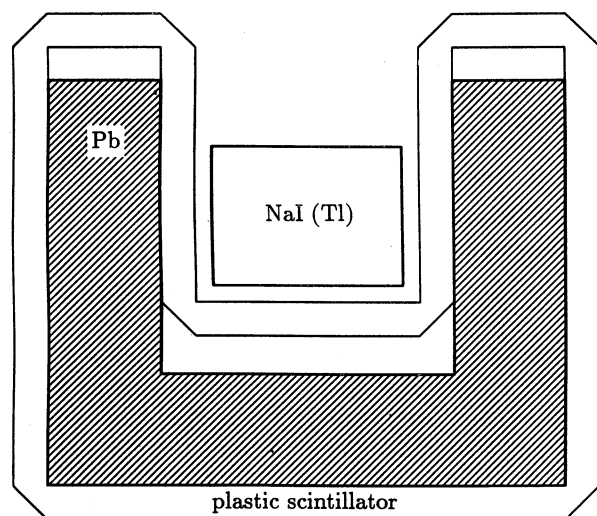


Fig. 1. Scheme of the detector-collimator system. In the diagram, the two photomultipliers have been omitted.

direct transmission for 500 keV photons of 0.7% and increasing then up to a maximum value of 25% for an energy between 3 to 4 MeV, for normal incidence.

In what follows, an estimate is made of the spectral characteristics of the radiation generated in the collimator, which emerges from its inner face. This way, a part of this radiation incides on the central scintillator and adds to the external radiation flux incident by the collimator aperture angle.

## 3. RADIATION ORIGINATED IN THE COLLIMATOR

During the balloon ascension through the atmosphere, and then at ceiling altitude, the different components of the secondary cosmic radiation (X-rays,  $\gamma$ -rays and also neutral and charged particles) incide on the collimator. A fraction of the incident photons of energy  $E$ , passes through the lead without undergoing interactions and is equal to  $I_0 \exp[-\mu(E)x]$  being  $I_0$  the intensity of the incident radiation,  $\mu(E)$  the total attenuation coefficient for gamma radiation of energy  $E$ , and  $x$  the path in the direction of incidence. Photons may interact in the material by means of three different processes: photoelectric, Compton, and pair creation.

High energy protons and neutrons interacting in the collimator, undergo nuclear interactions, producing in this way radioactive isotopes (Dyer & Morfill 1971), which when decaying, emit monochromatic gamma radiation, alpha particles, electrons, and positrons. When the interaction is initiated by a proton, the veto action of the plastic shielding should eliminate this event from the analysis, but the emission from the radioactive isotopes is produced with the characteristic isotope decay times, the event not being eliminated this way.

Thermal neutrons incident on the collimator, when captured by the different isotopes of Pb may produce emission of  $\gamma$ -rays and electrons, which also add to the instrumental background.

These three types of incident radiation: 1)  $\gamma$ -rays, 2) high energy electrons and protons, and 3) thermal neutrons, will be discussed below. The bremsstrahlung of electrons in the collimator will not be analyzed here, because its contribution is only important at lower energies.

### 3.1. Interactions of the Incident Gamma Radiation

The photons emerging from the inner face of the collimator, except those that are directly transmitted, are the result of successive interactions due to the relatively large thickness (a couple of interaction lengths thick for photons with an energy 20 MeV) of the lead wall, and will have lower energies than the incident photons.

When undergoing a photoelectric interaction, the

photon is absorbed. In the Compton interaction, the energy of the resulting photons has a continuum distribution given by the Klein-Nishina law (Heitler 1954), whereas a result of the pair electron-positron creation due to the incident photon, the subsequent positron annihilation generates two 511 keV photons. Each photon resulting from an interaction may, in turn, undergo another interaction and so on. That makes unpractical an analytic approach to the problem, so it is necessary to perform statistical simulation of the physical processes. In our case we use the Monte Carlo method, applied successfully in similar situations (Alder, Fernbach, & Rotenberg 1963; Stanton 1971; Martin, Bui Van, & Vedrenne 1971). We have included in this calculation not only the primary, but also the subsequent interactions, included secondary electrons.

We sampled the distribution function which describe probabilistically the different processes taking place in the event, by means of an "at random" choice of a number between 0 and 1. The procedures used are based in the general principles that give a foundation to the method (Cashwell & Everett 1959).

The Monte Carlo method is applied to determine: a) the direction of motion of the incident photon, b) the interaction length traversed before an interaction takes place, c) the type of interaction, and d) the energy and direction of the resulting photon.

For the computation, the following data inputs are given: a table with the cross sections values  $\sigma_{ph}(E)$ ,  $\sigma_c(E)$ , and  $\sigma_p(E)$  for each of the possible interactions (photoelectric, Compton, and pair creation, respectively), shape, dimensions, and density of the colli-

mator,  $E_i$  (energy of the incident photon), the direction  $C_o(I)$ , the point of incidence  $X_o(I)$  and the number of histories to analyze. During the computation random numbers are chosen between 0 and 1, which properly related with the corresponding distribution functions, allow us to determine with  $R_d$  the distance  $D$  to the next interaction and by means of  $D$  its position  $X(I)$ , with  $R_s$  the type of interaction produced at  $X(I)$ , by means of  $R_E$  the energy  $E$  of the resulting photon and with  $R_\theta$  and  $R_\phi$  the angles  $\theta$  and  $\phi$  that determine the direction of its motion.

The computation program used was prepared in order to give the photon spectrum emerging from the inner face of the collimator, in energy bins of width  $\Delta E = 10$  keV, when the energy of the incident photon is  $E_i < 10$  MeV and width  $\Delta E = 100$  keV for  $E_i > 10$  MeV.

Three cases of increasing complexity were studied by this method: a) infinite plane layer 3 cm thick, monochromatic incident radiation and normal incidence, b) infinite hollow cylinder 3 cm thick, monochromatic incident radiation and incidence direction normal to the cylinder axis, and c) infinite hollow cylinder 3 cm thick, monochromatic incident radiation with the incidence direction chosen randomly for an isotropic distribution. In the three cases eight different values of energy of the incident radiation were considered—between 1.25 and 95 MeV—and for each of them, 20 000 histories were analyzed.

The obtained results for the case c) which is the closest to the real conditions during the observations, are summarized in Table 1. From this table, it is evident that the average number of undergone interac-

TABLE 1

## RESULTS FOR THE CASE OF A HOLLOW INFINITE CYLINDER AND ISOTROPIC INCIDENCE

Parameter	Incident Photon Energy $E_i$ (MeV)							
	1.25	3.5	5.0	7.0	10.0	20.0	50.0	95.0
Num. emerg. phot. collimator inner face	1060	2122	1920	1746	1426	850	415	254
Num. phot. traver. collimator not interac.	532	1046	960	866	760	460	217	118
Num. phot. reemerging outer face	3304	6142	7004	7538	8392	9592	10934	11738
Num. 511 keV phot. emerg. inner face	4	122	156	176	188	144	90	98
Num. of Compton interactions	22740	24644	23090	22018	20656	18930	17905	16872
Num. photoelectric interactions	15900	18366	21050	22716	24386	26344	27166	26926
Num. pair creation interactions	264	6632	9974	12000	14204	16784	18515	18918

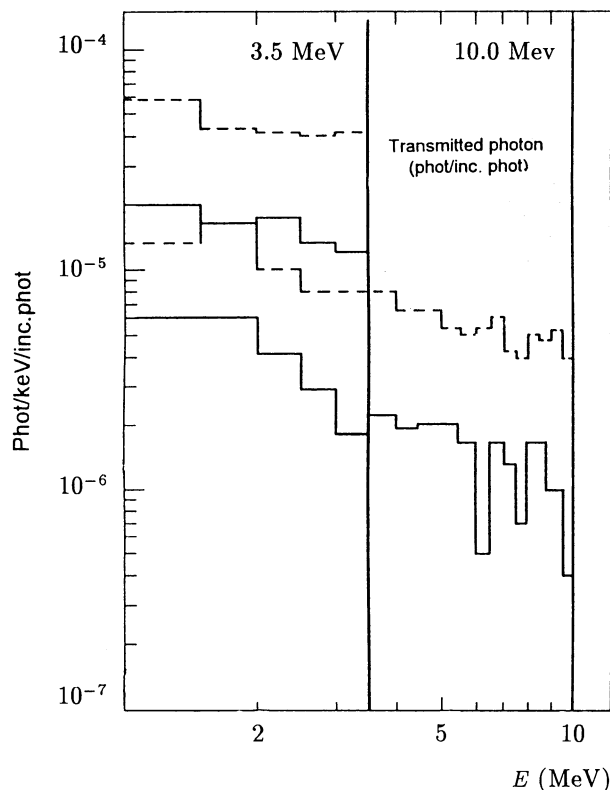


Fig. 2. Spectra emerging from the collimator inner face for incident photons of 3.5 and 10 MeV, obtained by the Monte Carlo method. The dashed line corresponds to case a (infinite plane layer 3 cm thick, monochromatic incident radiation with normal incidence). The full line corresponds to the case c (infinite hollow cylinder 3 cm thick, monochromatic incident radiation with isotropic incidence).

tions for each incident photon is about three and that only a small fraction of the numerous 511 keV photons produced by pair creation emerge from the inner face of the collimator. In Figure 2 two examples are shown of the emerging spectra from the inner face for cases a) and c) for incident photons with energies of 3.5 and 10 MeV. It should be noted that besides the production of a continuum background due to Compton interactions, a peak at 511 keV appears in both spectra and also at the energy  $E = E_i$ , corresponding this last peak to direct transmission. The peaks at 511 keV are not shown in Figure 2, due to the energy range displayed in the horizontal axis.

By using the results of the previous calculations, the contribution to the counting rate in the main detector due to the instrumental background generated in the collimator, can be estimated. To this end, a function called production function is defined. That function  $P(E_i, E)$  (photons  $\text{cm}^{-2}$  keV/incid photons

$\text{cm}^{-2}$ ) gives the number of photons of energy  $E$  per  $\text{cm}^2$  keV that emerge from the inner face due to each incident photon of energy  $E_i$  per  $\text{cm}^2$  in the outer face. This function is directly related to the values of the computation by the following relation

$$P(E_i, E) = \frac{A_e}{A_i} \frac{n(E_i, E)}{N(E_i)}, \quad (1)$$

where  $A_e$  and  $A_i$  are the outer and inner area of the collimator, respectively,  $n(E_i, E)$  is the number of photons with energy  $E$  per unit of energy, emerging due to the incidence of  $N(E_i)$  photons of energy  $E_i$ , being  $N(E_i)$  the number of histories used in the Monte Carlo method.

Analogously, the production function for the 511 keV line is given by

$$P(E_i, 511) = (A_e/A_i) \times n(E_i, 511)/N(E_i) \\ \text{phot cm}^{-2}/\text{incid phot cm}^{-2}. \quad (2)$$

In Figure 3, the relation  $n/N$  is shown for 1) the production of the 511 keV line, and 2) the continuum background. In the last case the average value of the photon production per unit of energy has been plotted. We can see from Figure 3, that the production of 511 keV photons is nearly constant for  $E_i > 3$  MeV and the average contribution to the continuum background decreases rapidly as  $E_i$  increases.

The relation between the number of photons that incide on the central detector through the aperture angle and those due to the instrumental background can be calculated through the production function. The ratio of counts must be greater than 1 to be sure that the instrumental background does not significantly affect the detector sensitivity. The exact computation of this number, considering the real geometrical configuration of the collimator-scintillator system would be too complicated. For the sake of simplicity we made an spherical approximation to the geometry of the collimator-scintillator system (see Figure 4).  $R_D$  is the radius of the supposed spherical detector,  $R_I$  and  $R_E$  are the internal and external radii of the assumed spherical collimator. The three radii have been chosen in such a way that the projected areas are equivalent to the mean projected areas, relative to an isotropic flux of the corresponding cylinders: detector and both inner and outer faces of the collimator. Estimates made for this spherical collimator show that the relation between the number of photons which incide through the aperture of the collimator and those due to the instrumental background is close to 10 at energies around 1 MeV and larger for higher energies, when an incident spectrum of the following form

$$dN/dE = 0.34 E^{-1.1} (\text{photons cm}^{-2} \text{s}^{-1} \text{MeV}^{-1}),$$

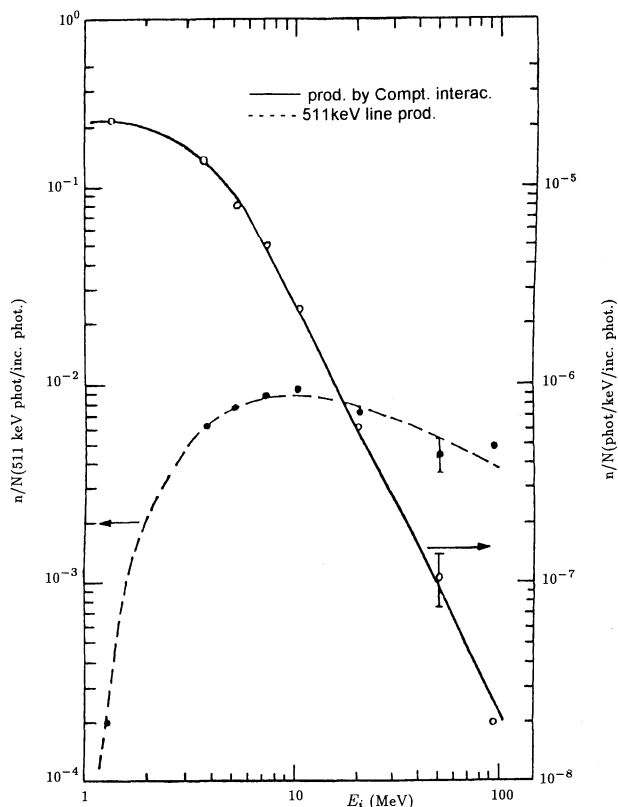


Fig. 3. Curves proportional to the production function for Compton interactions and the 511 keV line (produced by positron annihilation) obtained by the Monte Carlo method, for case c.

is considered. This form for the incident spectrum is given in a previous paper (Azcarate, Ghielmetti, & Mugerli 1992) and is derived from a measurement at the same place of the atmospheric gamma radiation, made with an uncollimated large plastic scintillator. The corresponding relation for the 511 keV line is slightly larger than unity.

### 3.2. Incident High Energy Protons and Neutrons

When the detector is in the atmosphere — at ceiling altitude — it is exposed to the incidence of primary protons with energies larger than the geomagnetic cut-off, which in our case corresponds to 11.1 GeV and secondary nucleons of energies of some hundreds of MeV. The computation of the production in the Pb, should combine the incident spectrum and the production cross section of each radioactive isotope. In what follows, it has been intended only to qualitatively analyze the different isotopes that can be generated in the lead when the material undergoes

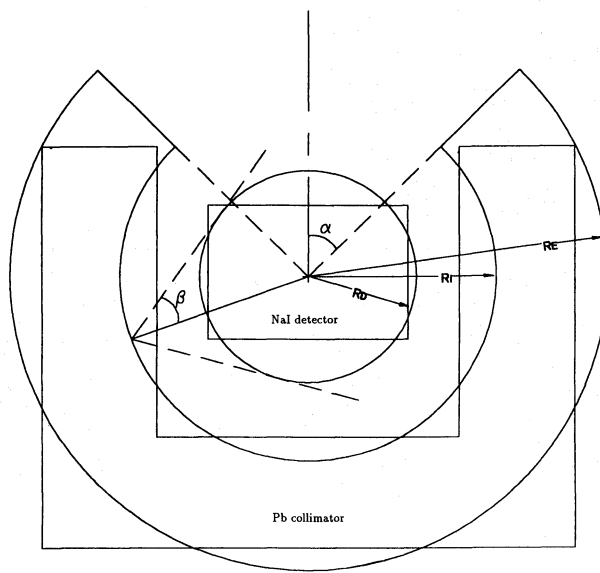


Fig. 4. Detector-collimator in the spherical approximation, superimposed on the real geometry of the system (the last one showed by a thinner line).

the action of cosmic rays, and the decay products of these isotopes. In particular, we were interested in the emission of gamma radiation and positrons which when annihilating contribute to the 511 keV peak.

The large value of the Pb mass number makes possible the generation of a large quantity of products of lower mass numbers. The production cross section for each of them may be calculated with a reasonable accuracy by the following formula given by Rudstam (1966)

$$\sigma(A, Z) = f_1(A_t) f_2(E) \times \frac{P \exp[-P(A_t - A)]}{1 - 0.3(PA_t)} \exp[-R | Z - Z_p |^{3/2}], \quad (3)$$

where  $A_t$  is the mass number of the target nucleus,  $E$  is the energy of the incident particle and  $A$  and  $Z$  are respectively the mass number and atomic number of the produced nucleus. The parameter  $P$ , which depends on the considered energy range,  $f_1$  and  $f_2$  are known. The same happens with the parameter  $R$  which slowly varies as a function of  $A$ . Besides,  $Z_p = SA - TA^2$  is the more probable atomic number for products with the same value of  $A$ , being  $T$  and  $S$  constant parameters.

The expression (3) shows that, on the one hand, the production cross section decreases in an exponential way as  $A$  departs from  $A_t$ , and on the other hand, for a product with a given  $A$ , decreases also exponentially when  $Z$  departs from  $Z_p$ .

TABLE 2

MOST IMPORTANT ISOTOPES PRODUCED IN Pb DUE TO  
NUCLEAR INTERACTIONS WITH HIGH ENERGY  
PROTONS AND NEUTRONS<sup>a</sup>

<i>A</i>	<i>Z</i>	Isotope	$\sigma_{rel}$	Lifetime	$E_{\gamma}$ (MeV)	$E_{\beta^+}$ (MeV)
207	84	Po <sup>m</sup>	1	2.8 s	0.26, 0.31, 0.82	...
207	84	Po	1	6 h	2.06	...
202	83	Bi	0.75	95 m	0.42, 0.96	...
201	82	Pb	0.71	61 s	0.63	...
199	82	Pb <sup>m</sup>	0.64	12.2 m	0.42	...
199	82	Pb	0.64	85 m	0.35, 0.37, 0.72	2.8 max
198	81	Tl <sup>m</sup>	0.60	1.9 h	0.28 - 0.64	...
198	81	Tl	0.60	5.3 h	... - 2.78	2.4 max
197	81	Tl <sup>m</sup>	0.57	0.54 s	0.38	...
197	81	Tl	0.57	2.84 h	0.426	...
196	81	Tl <sup>m</sup>	0.53	1.41 h	0.43	...
196	81	Tl	0.53	1.84 h	0.426	...
193	80	Hg	0.45	5.0 h	1.08	...
192	79	Au	0.42	4.1 h	1.2	...
191	79	Au	0.40	3.2 h	0.60	...
184	77	Ir	0.27	3.2 h	4.3	...
203	82	Pb	0.27	6.1 s	0.82	...
202	82	Pb	0.25	3.62 h	0.96	...
180	75	Ro	0.22	2.4 m	0.511, 0.88	...

<sup>a</sup> Main decay products are also given.

From the table of isotopes (Lederer, Hollander, & Perlman 1967), we have taken the radioactive products, and calculated by the expression (3) the cross sections relative to that of the Po<sup>207</sup>, which is approximately 3200 mbarns.

In Table 2 the more important isotopes are given in order of decreasing cross sections, all of them meeting the requirement that its lifetime is shorter than 9 hours. On the right side of the table the energies of the  $\beta^+$  and  $\gamma$  emissions are given. From the results of the gamma emission it is derived that, excepting some isolated cases, the  $\gamma$ -rays energies are lower than 1 MeV.

### 3.3. Thermal Neutron Interactions

The radioactive capture of slow neutrons by the Pb nuclei (Siegbahn 1968) gives as a main result the emission of monoenergetic photons. We show in Table 3 for each of the isotopes composing the natural Pb, the capture cross section, lifetime of the products and gamma radiation emitted by the Pb, due to the thermal neutron capture (Lederer et al. 1967). From the analysis of the results given in Table 3, it is evident that only from the capture by

the isotope Pb<sup>206</sup> there might be an important contribution to the instrumental background, for  $\gamma$ -ray energies slightly larger than 1 MeV. The values corresponding to the same processes in Na<sup>23</sup> and I<sup>127</sup> (elements composing the central scintillator) are also given in Table 3, together with the total number of atoms of each species that are contained in both the scintillator and the collimator. We can see that the capture cross section of I<sup>127</sup> is more than 200 times larger than that of the Pb<sup>206</sup>, whereas the number of atoms of Pb<sup>206</sup> is only 10 times larger than for I<sup>127</sup>. This indicates that there is a larger production in the scintillator than in the collimator. Therefore, the instrumental background will not be increased considerably by the presence of the collimator, as far as the neutron capture process is concerned.

## 4. EXPERIMENTAL TEST

The detector system analyzed here, was experimentally tested during a balloon flight carried out on 18 November 1973, from Paraná, provincia de Entre Ríos, Argentina. The balloon stayed at ceiling altitude (36 km) during about 8 hours. The balloon volume was 85 000 m<sup>3</sup>. Energy loss spectra produced

TABLE 3

NEUTRON CAPTURE CROSS SECTIONS, LIFETIME OF THE PRODUCTS  
AND RADIATIONS EMITTED IN THEIR DECAY FOR LEAD, SODIUM AND IODINE

Isotope	%	$\sigma_{capt}$ (barns)	Lifetime	$E_{\gamma}$ (MeV)	$E_{elect}$ (MeV)	No. Nuclei in the Detector ( $10^{24}$ )
Pb <sup>204</sup>	1.5	0.7	$3.10^7$ y	X-rays	...	0.64
Pb <sup>206</sup>	25.0	0.03	0.8 s	0.57, 1.06	0.48, 0.98	10.7
Pb <sup>207</sup>	21.5	0.72	...	...	...	9.2
Pb <sup>208</sup>	52.0	$5.10^{-4}$	3.3 h	No $\gamma$ -rays	0.64 max	22.0
Na <sup>23</sup>	100	0.53, 0.40	15 h, 0.02 s	1.37, 2.75, 0.472	4.17, 6.0 m	1.15
I <sup>127</sup>	100	6.4	25 m	X-rays, 0.44–0.97	2.2 max	1.15

in the central scintillator were taken during the ascension and at ceiling altitude. A sample of the observed spectra, at ceiling altitude, is shown in Figure 5, covering an energy range from 0.3 to 8 MeV. The detected photons belong partially to the atmospheric background. The atmospheric photons either incide directly through the aperture of the collimator or pass through the collimator without interacting. To this component add the energy degraded photons that emerge from the inner face of the collimator. It is a rather difficult task to derive from this measurement the shape and intensity of the incident spectrum—given the crystal-collimator configuration—which has an energy-dependent geometrical factor. Besides, Compton interactions in lead modified the shape of the  $\gamma$ -ray spectrum inciding on the central detector. In addition to this, we do not have a precise knowledge of the response function of the crystal, which relates the observed pulse spectrum to the incident  $\gamma$ -ray spectrum.

Martin (1975) computed the response function for a NaI crystal with same dimensions to ours, but uncollimated, by using a Monte Carlo calculation. His obtained energy-loss spectrum was similar to ours in the energy range 2–4 MeV, when considering an incident  $\gamma$ -ray spectrum similar to that measured in other experiment with a large uncollimated plastic scintillator (Azcarate et al. 1992). This agreement would indicate that the induced instrumental background is negligible for the range 2–4 MeV. For the energies  $< 2$  MeV, we see from Figure 5 an additional component, above the extrapolated energy loss spectrum. This excess would be the instrumental background generated by nuclear interactions in Pb and in the NaI (Tl) itself. It should be noted that, even though the gamma radiation emitted by the radioactive products is monoenergetic, the successive interactions undergone in the collimator give as a result a continuum background.

The presence of a peak corresponding to the 511 keV line, resulting from positron annihilation is observed in the spectrum. To the atmospheric component of this line add the contribution generated in the collimator. By using our Monte Carlo computa-

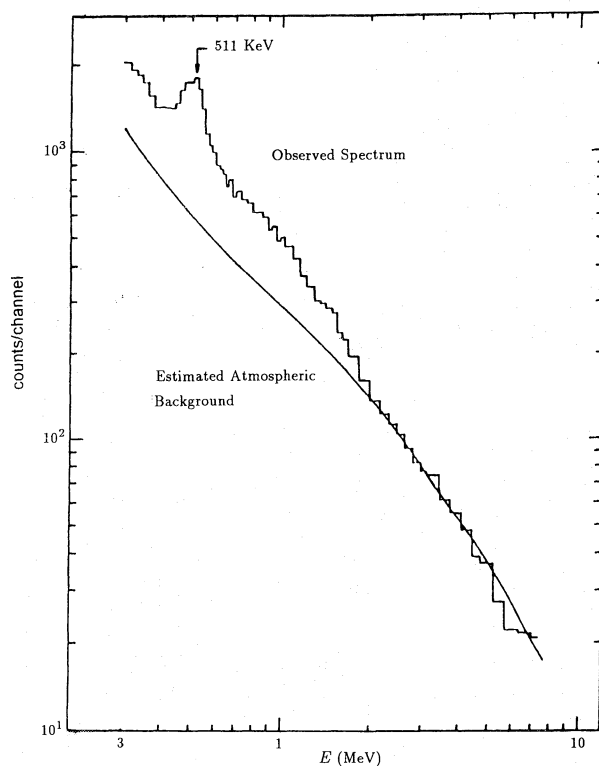


Fig. 5. Observed pulse spectrum in the central scintillator, at an atmospheric depth of  $4.5 \text{ g cm}^{-2}$  (altitude 36 km) taken during 124 minutes, on the 18 November 1973 balloon flight.

tions, we can estimate that the instrumental background for the 511 keV line is about 50% of the total intensity. Therefore, even in this particular region of the spectrum, the collimator does not significantly affect the detector sensitivity.

From the observed spectra at ceiling altitude, the atmospheric 511 keV line flux results to be  $(9.0 \pm 0.7) \times 10^{-2}$  photons  $\text{cm}^{-2} \text{s}^{-1}$ , in very good agreement with measurements carried out at places with different geomagnetic cut-offs (Albernhe & Vedrenne 1979; Mahoney, Ling, & Jacobson 1981; Kasturirangan, Rao, & Bhavsar 1972).

### 5. SUMMARY

In the case of the 511 keV line, the presence of the collimator reduces the geometric factor of the detector by a factor of 5 (for an isotropic background flux), whereas the intensity of the line generated in the Pb is almost equal to that of the atmospheric origin.

For energies  $< 2$  MeV, other than 511 keV, there is an induced continuum instrumental background, mainly produced by nuclear interactions in Pb and in NaI.

For the range of energies  $E > 2$  MeV, both the computation and the observation indicate that the instrumental background is negligible and, besides, that the collimator reduces the geometrical factor for an isotropic flux by a factor of 3. In short, the presence of the collimator did not significantly affect the measurement of the atmospheric 511 keV line and improved the detector sensitivity in the energy range  $E > 2$  MeV of the spectrum for gamma radiation lines from astronomical sources, such as 2.23, 4.43 and 6.13 MeV lines (Ramaty, Kozlovsky, & Lingenfelter 1979). These three lines have been detected in several solar flares (Chupp et al. 1973; Chupp 1990), being the 2.23 MeV line originated in capture of neutron on hydrogen, while the 4.43 and 6.13 MeV

lines, in de-excitation of excited  $^{12}\text{C}$  and  $^{16}\text{O}$ , respectively. These last two lines have been also detected by COMPTEL on board the *GRO* satellite, from the Orion complex (Bloemen et al. 1994).

### REFERENCES

- Albernhe, F., & Vedrenne, G. 1979, *J. Geophys. Res.*, 84, 6658
- Alder, B., Fernbach, S., & Rotenberg, M. 1963, *Methods in Computational Physics*, Vol. 1 (New York: Academic Press)
- Azcarate, I.N., Ghielmetti, H.S., & Mughlerli, V.J. 1992, *Ap&SS*, 190, 317
- Bloemen, H. et al. *A&A*, 281, L5
- Cashwell, E.D., & Everett, C.J. 1959, *A Manual of the Monte Carlo Method for Random Walk Problems* (New York: Pergamon Press)
- Chupp, E.L. 1990, *ApJS*, 73, 213
- Chupp, E.L., Forrest, D.J., Higbie, P.R., Suri, A.N., Tsai, C., & Dunphy, P.P. 1973, *Nature*, 241, 333
- Dyer, C.S. & Morfill, G.E. 1971, *Ap&SS*, 14, 243
- Heitler, W. 1954, *The Quantum Theory of Radiation* (Oxford: Clarendon Press)
- Kasturirangan, K., Rao, U., & Bhavsar, P. 1972, *Planet Space Sci.*, 20, 1961
- Lederer, C.M., Hollander, J.M., & Perlman, I. 1967, *Table of Isotopes* (New York: John Wiley and Sons Inc.)
- Mahoney, W.A., Ling, J.C., & Jacobson, A.S. 1981, *J. Geophys. Res.*, 86, 11098
- Martin, I.M. 1975, private communication
- Martin, I.M., Bui Van, A., & Vedrenne, G. 1971, *Nuclear Instruments and Methods*, 95, 545
- Rudstam, G. 1966, *Z. Naturforschg*, 21, 1027
- Ramaty, R., Kozlovsky, B., & Lingenfelter, R.E. 1979, *ApJS*, 40, 487
- Siegbahn, K. 1968, *Beta and Gamma-ray Spectroscopy*, 1, 769 (Amsterdam: North-Holland Publishing Co.)
- Stanton, N.R. 1971, *A Monte Carlo Program for Calculating Neutron Detection Efficiencies in a Plastic Scintillator*, C00-1545-72, (Columbus, Ohio: The Ohio State University)

Ismael N. Azcárate: Instituto Argentino de Radioastronomía, Casilla de Correo No. 5, Villa Elisa (1894), Prov. de Buenos Aires, Argentina. (azcarate@irma.edu.ar).

Vicente J. Mughlerli: Comisión Nacional de Actividades Espaciales, Paseo Colón No. 751, (1063) Buenos Aires, Argentina.